Size-Selective Surface Silylation of Cagelike Mesoporous Silica SBA-2 with Disilazane Reagents

Clemens Zapilko and Reiner Anwander*

Department of Chemistry, Universitetet i Bergen, Allégaten 41, N-5007 Bergen, Norway

Received November 4, 2005. Revised Manuscript Received January 19, 2006

Dehydrated, structurally ordered silica materials SBA-1 and SBA-2 were reacted with two differently sized silylamines, tetramethyldisilazane ($HN(SiHMe_2)_2$) and tetramethyldiphenyldisilazane ($HN(SiMe_2Ph)_2$), at ambient temperature. The intraporous silylation is controlled by the different sizes of the pore entrances/cage windows of these "mesoporous" silica materials. According to nitrogen physisorption, Fourier transform infrared spectroscopy, and carbon elemental analysis, the vast majority of the channels and pore openings, interconnecting the supercages of SBA-2 ($P6_3/mmc$), display a diameter larger than the size of a $HN(SiHMe_2)_2$ molecule (silylation efficiency, SE, 1.98−2.28 mmol $SiHMe_2$/1 g); however, this is smaller than that of a $HN(SiMe_2Ph)_2$ molecule (SE, 0.40−0.63 mmol $SiMe_2Ph$/1 g). The inner surface of SBA-1 (space group $Pm3n$) is fully accessible to both disilazane reagents giving SE values of 4.03 mmol $SiHMe_2$/1 g and 2.91 mmol $SiMe_2Ph$/1 g. The lower SE value for material $SiMe_2Ph$@SBA-1 reflects the increased steric bulk of the silylating reagent which hampers the silylation of neighbored silanol functional groups.

Introduction

Periodic mesoporous silica materials featuring a three-dimensional interconnected pore system are likely to show enhanced pore accessibility and more efficient mass transport through the internal pore volume compared to two-dimensional structures such as MCM-41 and SBA-15,[1] which is beneficial for applications in catalysis and chemical sensoring.[2] Three-dimensional mesoporous silicas comprise MCM-48, which possesses a pore network consisting of two interpenetrating channel systems,[3] and materials with cagelike mesopores such as KIT-5,[4] FDU-1,[5] AMS-1,[6] AMS-2,[7] AMS-8,[7] and members of the SBA-series including SBA-1,[8] SBA-6,[9] SBA-2,[10] SBA-12,[11] and SBA-16.[12] These silica phases feature periodic arrays of spherical supercages in a 3−10 nm range which are interconnected by narrow channels or windows. Jaroniec et al. showed for SBA-16[13] and FDU-1[14] that the size of the channels can be effectively tailored in a range from <1 to 6 nm by properly adjusting the synthesis conditions. This feature makes cagelike silicas promising candidates for shape/size selective catalysis and adsorbents involving molecules, which are too large to diffuse into zeolitic materials. SBA-1[9] (space group $Pm3n$) and SBA-2[11] ($P6_3/mmc$) were initially synthesized by Huo et al., and their pore structure was elucidated by electron crystallography and high-resolution transmission electron microscopy.[11,15] Information about the interconnecting channels was obtained from adsorption studies with differently sized hydrocarbons by the Wright group.[16] Accordingly, 0.4−1.5 nm pore openings are typical of SBA-2 materials, while SBA-1 silica tends to accommodate larger channels. Furthermore, Monte Carlo simulations of the adsorption behavior of methane and ethane in SBA-2 revealed that a distribution of the channel size has to be considered.[17]

The objective of the present study was to test the feasibility of size selective surface functionalization of cagelike mesoporous silicas SBA-1 and SBA-2. Such reactions would provide a simple method to estimate the size of the pore openings and simultaneously to tune the mesopore accessibility. Suface silylations with chloro-, alkoxy-, or aminosi-

* To whom correspondence should be addressed. Phone: +4755589491. Fax: +4755589490. E-mail: anwander.reiner@kj.uib.no.

(1) (a) Kresge, C. T.; Leonowicz, M. E.; Roth, W. J.; Vartuli, J. C.; Beck, J. S. *Nature* **1992**, *359*, 710. (b) Zhao, D.; Feng, J.; Huo, Q.; Melosh, N.; Fredrickson, G. H.; Chmelka, B. F.; Stucky, G. D. *Science* **1998**, *279*, 548.
(2) (a) Morey, M. S.; Davidson, A.; Stucky, G. D. *J. Porous Mater.* **1998**, *5*, 195. (b) Che, S.; Sakamoto, Y.; Terasaki, O.; Tatsumi, T. *Chem. Mater.* **2001**, *13*, 2237. (c) Liu, M.-C.; Sheu, H.-S.; Cheng, S. *Chem. Commun.* **2002**, 2854.
(3) Kaneda, M.; Tsubakiyama, T.; Carlsson, A.; Sakamoto, Y.; Ohsuna, T.; Terasaki, O.; Joo, S. H.; Ryoo, R. *J. Phys. Chem. B* **2002**, *106*, 1256.
(4) Kleitz, F.; Liu, D.; Anilkumar, G. M.; Park, I.-S.; Soloviov, L. A.; Shmakov, A. N.; Ryoo, R. *J. Phys. Chem. B* **2003**, *107*, 14296.
(5) Yu, C.; Yu, Y.; Zhao, D. *Chem. Commun.* **2000**, 575.
(6) Che, S.; Garcia-Bennett, A. E.; Yokoi, T.; Sakamoto, K.; Kunieda, H.; Terasaki, O.; Tatsumi, T. *Nature Mat.* **2003**, *2*, 801.
(7) Garcia-Bennett, A. E.; Miyasaka, K.; Terasaki, O.; Che, S. *Chem. Mater.* **2004**, *16*, 3597.
(8) Huo, Q.; Margolese, D. I.; Stucky, G. D. *Chem. Mater.* **1996**, *8*, 1147.
(9) Sakamoto, Y.; Kaneda, M.; Terasaki, O.; Zhao, D. Y.; Kim, J. M.; Stucky, G.; Shin, H. J.; Ryoo, R. *Nature* **2000**, *408*, 449.
(10) Huo, Q.; Margolese, D. I., Leon, R.; Petroff, P. M.; Stucky, G. D. *Science* **1995**, *268*, 1334.
(11) Kruk, M.; Jaroniec, M.; Ryoo, R.; Kim, J. M. *Chem. Mater.* **1999**, *11*, 2568.
(12) Zhao, D.; Huo, Q.; Feng, J.; Chmelka, B. F.; Stucky, G. D. *J. Am. Chem. Soc.* **1998**, *120*, 6024.
(13) Kim, T.-W.; Ryoo, R.; Kurk, M.; Gierszal, K. P.; Jaroniec, M.; Kamiya, S.; Terasaki, O. *J. Phys. Chem. B* **2004**, *108*, 11480.
(14) Kruk, M.; Antochshuk, V.; Matos, J. R.; Mercuri, L. P.; Jaroniec, M. *J. Am. Chem. Soc.* **2002**, *124*, 768.
(15) Zhou, W.; Hunter, H. M. A.; Wright, P. A.; Ge, Q.; Thomas, J. M. *J. Phys. Chem. B* **1998**, *102*, 6933.
(16) Garcia-Bennett, A. E.; Williamson, S.; Wright, P. A.; Shannon, I. J. *J. Mater. Chem.* **2002**, *12*, 3533.
(17) (a) Perez-Mendoza, M.; Gonzalez, J.; Wright, P. A.; Seaton, N. A. *Langmuir* **2004**, *20*, 7653. (b) Perez-Mendoza, M.; Gonzalez, J.; Wright, P. A.; Seaton, N. A. *Langmuir* **2004**, *20*, 9856.

10.1021/cm0524345 CCC: $33.50 © 2006 American Chemical Society
Published on Web 02/22/2006

lanes are well-known procedures for the pore size engineering of zeolites.[18] The reaction of disilazanes $HN(SiR_3)_2$ with surface silanol groups of MCM-41 has already been studied in detail.[19]

Experimental Section

General Materials. Tetraethyl orthosilicate (TEOS) from Fluka was used as a silica precursor. Mesitylene (TMB) and tetramethylammonium hydroxide (25 wt % solution in water, TMAOH) were purchased from Aldrich. Silylation reactions were performed under dry argon using glovebox techniques (MB Braun MBLab; <1 ppm O_2, <1 ppm H_2O). Hexane was purifed by using Grubbs columns (MBraun SPS, solvent purification system) and stored in a glovebox. 1,1,3,3-Tetramethyldisilazane and 1,3-diphenyl-1,1,3,3-tetramethyldisilazane were obtained from Gelest. The reagents were used as received without further purification. Octadecyltriethylammonium bromide $[CH_3(CH_2)_{17}NEt_3]^+Br^-$ (C_{18}TEABr) and divalent surfactant *N*-(3-trimethylammoniumpropyl)hexadecylammonium dibromide $[CH_3(CH_2)_{15}NMe_2(CH_2)_3NMe_3]^{2+}2Br^-$ (C_{16-3-1}) were synthesized according to the literature by reacting octadecylbromide with triethylamine and hexadecyldimethylamine with (3-bromopropyl)-trimethylammonium bromide, respectively.[20,21]

SBA-1. C_{18}TEABr (5.00 g, 11.47 mmol), concentrated HCl (37 wt %, 318 g, 2.79 mol), and distilled water (525 g, 29.17 mol) were combined, and the resulting mixture was vigorously stirred until a homogeneous solution formed (ca. 30 min). The solution was cooled to 0 °C in an ice bath, and 12.00 g (57.60 mmol) of TEOS was slowly added. Stirring was continued for 4 h at 0 °C, and then the reaction mixture was heated in a polypropylene bottle to 100 °C and maintained there for 1 h without stirring. The solid product was recovered by filtration (without washing) and dried at ambient temperature. The as-synthesized material was calcined at 540 °C (air, 5 h) and dehydrated in vacuo (270 °C, 10^{-4} Torr, 4 h). The molar composition of the synthesis gel was 1:5:280:3500 C_{18}TEABr/TEOS/HCl/H_2O.

SBA-2a. A total of 10 g of TMAOH (27.44 mmol, 25 wt % in water) and 1 g (2.74 mmol) C_{16-3-1} were dissolved in 140 g of water, and the mixture was stirred until a clear solution formed (ca. 30 min). TEOS (11.43 g, 54.87 mmol) was added over a period of 5 min, and the resulting synthesis mixture was stirred at 25 °C for 2 h. The material was recovered by filtration, washed several times with distilled water, air-dried overnight at ambient temperature, calcined at 540 °C, and finally dehydrated in vacuo (270 °C, 10^{-4} Torr, 4 h). The molar composition of the synthesis gel was 1:20:10:3000 C_{16-3-1}/TEOS/TMAOH/H_2O.

SBA-2b. The synthesis was similar to the procedure outlined above for SBA-2a; however, 3.98 g (32.92 mmol) of TMB was added to the synthesis mixture prior to the addition of TEOS. The molar composition of the synthesis gel was 1:20:10:0.6:3000 C_{16-3-1}/TEOS/TMAOH/TMB/H_2O.

Surface Silylation of SBA-1 and SBA-2a/b. The silylation reactions were carried out by adding the disilazane reagent diluted in 2 mL of hexane to 0.20 g of dehydrated mesoporous silica suspended in about 5 mL of hexane. After stirring the reaction mixture for a desired period of time (18 h for SBA-1, 3 days for SBA-2) at ambient temperature, unreacted disilazane was separated by several hexane washings via centrifugation. The silylated materials were dried under vacuum for 3 h at 20 °C and then heated at 250 °C under high vacuum for 3 h.

Characterization. Powder X-ray diffraction (PXRD) patterns were recorded on a Philips X'pert PRO instrument in the step/scan mode (step width, 0.034; accumulation time, 30 s/step; range (2θ), 0.31−9.96°) using monochromatic Cu Kα radiation ($\lambda = 1.5418$ Å). IR spectra of the parent and silylated materials were recorded on a Perkin-Elmer Fourier transform infrared (FTIR) spectrometer 1760X using Nujol mulls sandwiched between CsI plates. Nitrogen adsorption−desorption isotherms were measured with an ASAP 2020 volumetric adsorption apparatus (Micromeritics) at 77.4 K for relative pressures from 10^{-2} to 0.99 [$a_m(N_2, 77\ K) = 0.162$ nm^2]. Prior to analysis, the samples were outgassed in the degas port of the adsorption analyzer at 523 K for 3 h. The BET specific surface area was obtained from the nitrogen adsorption data in the relative pressure range from 0.04 to 0.20.[22] The pore size distributions were derived from the desorption branch using the Barrett−Joyner−Halenda (BJH) method.[23] Although the BJH method systematically underestimates the effective pore diameter of materials,[24−26] it gives a good measure of relative changes of the pore size. Herein, we made use of this method to determine the pore diameter of our cagelike silicas. In addition, the cage diameters of the parent materials were calculated using equation $D_{me} = a(6\epsilon_{me}/\pi\upsilon)^{1/3}$, which has been proposed by Ravikovitch and Neimark.[25] D_{me} is the diameter of the cavities of a cubic unit cell of length a, $\epsilon_{me} = \rho_v V_{me}/(1 + \rho_v V_{me})$ is the volume fraction of a regular cavity, where $\rho_v = 2.2$ g cm^{-3} is the estimated silica wall density, and υ is the number of cavities per unit cell (for the *Pm*3*n* space group, $\upsilon = 8$). Elemental analyses were performed on an Elementar VarioEL/Perkin-Elmer instrument. The surface silanol population was obtained from the surface coverage $\alpha(SiR_3)$ of activated silylated samples as described previously.[19a]

Results and Discussion

Mesoporous silica materials SBA-1, SBA-2a, and SBA-2b were synthesized according to slightly modified literature procedures.[27,28] PXRD analysis of the calcined materials revealed a larger unit cell dimension for SBA-2b (168 nm^3) compared to that of SBA-2a (121 nm^3; Figure 1). Correspondingly, N_2 physisorption and application of the BJH

(18) For examples, see: (a) Hdasama, C. D.; Sebastian, J.; Jasra, R. V. *Ind. Eng. Chem. Res.* **2005**, *44*, 1780. (b) Huttenloch, P.; Roehl, K. E.; Czurda, K. *Environ. Sci. Technol.* **2001**, *35*, 4260. (c) Galletero, M. S.; Corma, A.; Ferrer, B.; Fornes, V.; Garcia, H. *J. Phys. Chem. B* **2003**, *107*, 1135.
(19) (a) Anwander, R.; Nagl, I.; Widenmeyer, M.; Engelhardt, G.; Groeger, O.; Palm, C.; Röser, T. *J. Phys. Chem. B* **2000**, *104*, 3532. (b) Jentys, A.; Pham, N. H.; Vinek, H. J. *Chem. Soc. Faraday Trans.* **1996**, *92*, 3287.
(20) Zana, R.; Benrraou, M.; Rueff, R. *Langmuir* **1991**, *7*, 1072.
(21) Widenmeyer, M. Ph.D. Thesis, Technische Universität München, München, 2001.
(22) (a) Brunauer, S.; Emmett, P. H.; Teller, E. *J. Am. Chem. Soc.* **1938**, *60*, 309. (b) Sing, K. S. W.; Everett, D. H.; Haul, H. R. A. W.; Moscou, L.; Pierotti, R. A.; Rouquérol, J.; Siemieniewska, T. *Pure Appl. Chem.* **1985**, *57*, 603.
(23) Barrett, E. P. Joyner, L. G. Halenda, P. P. *J. Am. Chem. Soc.* **1951**, *73*, 373.
(24) Kruk, M.; Jaroniec, M.; Sayari, A. *Chem. Mater.* **1999**, *11*, 492.
(25) (a) Ravikovitch, P. I.; Domhnaill, S. C. O.; Neimark, A. V.; Schüth, F.; Unger, K. K. *Langmuir* **1995**, *11*, 4765. (b) Ravikovitch, P. I.; Wei, D.; Chueh, W. T.; Haller, G. L.; Neimark, A. V. *J. Phys. Chem. B* **1997**, *101*, 3671. (c) Ravikovitch, P. I. Neimark, A. V. *Langmuir* **2000**, *16*, 2419.
(26) Lukens, W. W., Jr.; Schmidt-Winkel, P.; Zhao, D.; Feng, J.; Stucky, G. D. *Langmuir* **1999**, *15*, 5403.
(27) Kim, M. J.; Ryoo, R. *Chem. Mater.* **1999**, *11*, 487.
(28) Hunter, H. M. A.; Wright, P. A. *Microporous Mesoporous Mater.* **2001**, *43*, 361.
(29) Ravikovitch, P. I.; Neimark, A. V. *Langmuir* **2002**, *18*, 1550.
(30) Note that the application of disilazane reagents implicating a monofunctional surface reaction is crucial for this study because alkoxy- and chlorosilanes exhibit sluggish and multifunctional reactions with silanol species.

Table 1. Pore Parameters and Carbon Content of Parent Silica and Silylated SBA-2 and SBA-1 Materials

sample[a]	a_s(BET)[b] ($m^2\ g^{-1}$)	V_{tot}[c] ($cm^3\ g^{-1}$)	$d_{p,ads}$[d] (nm)	$d_{p,des}$[d] (nm)	C[e] (%, w/w)	SiR_3[e] (mmol g^{-1})
SBA-1	1470	0.84	2.4	2.2		
SBA-2a	850	0.58	2.5	2.4		
SBA-2b	1010	0.69	2.6	2.6		
$SiHMe_2$@SBA-1 (**3**)	780	0.38	1.8	1.6	7.85	4.03
$SiHMe_2$@SBA-2a (**5**)	740	0.47	2.4	2.4	4.26	1.98
$SiHMe_2$@SBA-2b (**6**)	780	0.51	2.3	2.2	4.84	2.28
$SiMe_2Ph$@SBA-1 (**4**)	570	0.25	1.7	1.5	20.08	2.91
$SiMe_2Ph$@SBA-2a (**7**)	800	0.52	2.4	2.4	3.66	0.40
$SiMe_2Ph$@SBA-2b (**8**)	860	0.57	2.6	2.5	5.54	0.63

[a] Pretreatment temperature 250 °C; 3 h; 10^{-3} Torr. [b] Specific BET surface area. [c] BJH desorption cumulative pore volume of pores between 15 and 200 Å diameter. [d] Pore diameter according to the maximum of the BJH adsorption/desorption pore size distribution; d_p values < 2.0 nm resulting from BJH method have to be viewed critically. [e] Corrected carbon content from elemental analysis and silyl group population calculated therefrom.

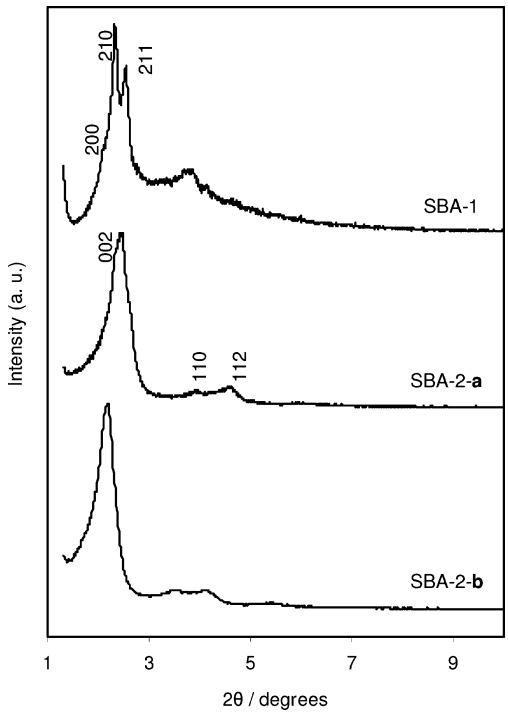

Figure 1. PXRD pattern of calcined mesoporous silicas.

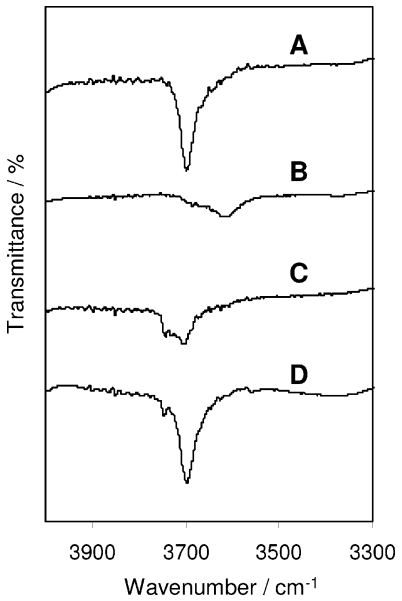

Figure 2. Region of the OH stretch vibration of SBA-2a (A), $SiMe_2$-Ph@SBA-1 (B), $SiHMe_2$@SBA-2a (C), and $SiMe_2Ph$@SBA-2a (D). The IR spectra were recorded as a Nujol mull.

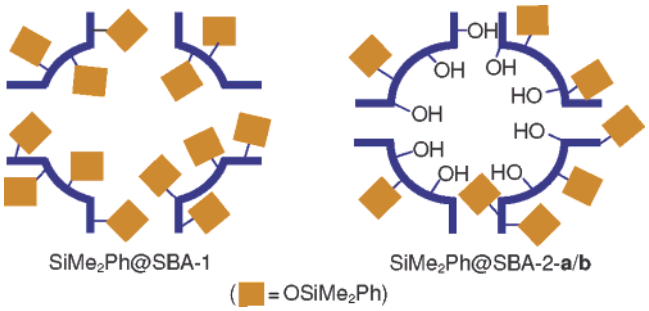

Figure 3. Schematic drawing of dimethylphenyl silylated SBA materials.

method indicated the largest pore diameter for SBA-2b (d_p = 2.6 nm, Table 1; Supporting Information). The pore diameters of the SBA-1 and SBA-2a/b cavities were calculated as 4.5 and 4.4/4.6 nm, respectively, using an equation which was recently proposed by Ravikovitch and Neimark.[29]

For the silylation reactions, tetramethyldisilazane $HN(SiHMe_2)_2$ (**1**) and tetramethyldiphenyldisilazane $HN(SiMe_2Ph)_2$ (**2**) were used as differently sized probe molecules.[30] The surface reactions were easily monitored by FTIR spectroscopy (samples were prepared as Nujol mulls). The unmodified parent materials exhibited a sharp band at 3695 cm^{-1} for the OH stretching mode of isolated surface silanol groups (Figure 2A). Reaction of SBA-1 with $HN(SiHMe_2)_2$ (**1**), affording hybrid material $SiHMe_2$@SBA-1 (**3**), consumed all of the IR detectable OH groups within 18 h. The band at 3695 cm^{-1} disappeared completely, and a new signal at 2145 cm^{-1} appeared as a result of the SiH stretching vibration of $\equiv Si-O-SiHMe_2$ surface sites (not shown). Carbon elemental analysis of this material corresponds to a silyl group population of 4.03 mmol g^{-1} or 2.14 $SiHMe_2$/1 nm^2 (Table 1). Similar observations were made for the silylation of SBA-1 with $HN(SiMe_2Ph)_2$ (**2**), resulting in $SiMe_2Ph$@SBA-1 (**4**; Figures 2B and 3). The sharp OH band disappeared, and a number of new signals at 3073, 3053, 1597, 833, 795, and 700 cm^{-1} indicative of silicon attached phenyl groups were detected. In the OH region of the spectrum only a broad band centered at 3616 cm^{-1} was observed. This band is assigned to a minor amount of unreacted SiOH groups, which are shielded by neighboring phenyl rings.[19a] Apparently, the SBA-1 pore system is fully accessible to both silylating reagents, and, hence, the channels connecting the mesocages are larger than the cross section of a $HN(SiPhMe_2)_2$ molecule (ca. 1.3 × 0.6 nm).

The corresponding silylation experiments with materials SBA-2a and and SBA-2b gave completely different findings.

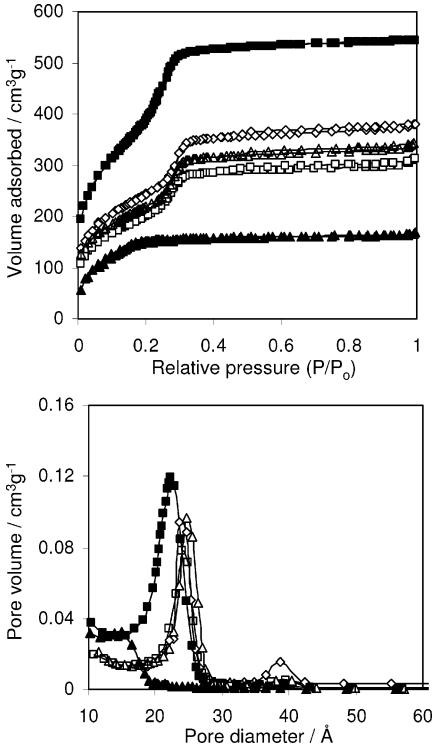

Figure 4. Nitrogen adsorption/desorption isotherms and corresponding BJH pore size distributions of the parent (SBA-1, ■; SBA-2a, ◇) and silylated materials ($SiHMe_2$@SBA-2a (**5**), □; $SiMe_2Ph$@SBA-2a, △; $SiMe_2Ph$@SBA-1 (**4**), ▲).

When treated with $HN(SiHMe_2)_2$ (**1**) for 3 days, both materials still indicated a considerable amount of nonreacted OH groups (Figure 2C). Consequently, the internal pore volume of SBA-2 materials seems to be only partially accessible even to a relatively small-sized molecule **1** (ca. 0.8×0.5 Å). Interestingly, in materials $SiHMe_2$@SBA-2a/b (**5**/**6**), the original OH band at 3695 cm^{-1} is split into two peaks with maxima at 3745 and 3695 cm^{-1}. While the latter signal is typical of isolated silanol groups if the silica sample is prepared as a Nujol mull, the band at 3745 cm^{-1} is characteristic of the same moiety, if the spectrum is recorded under vacuum conditions.[19b] We assume that a marked portion of the pore openings of SBA-2 is blocked upon reaction with **1**, thus, counteracting the wetting of the internal surface area by the mineral oil used for the mull preparation. Such cage-confined silanol groups give rise to the observed blue shift of the OH stretching frequency. The size-selective surface silylation is corroborated by the reaction of SBA-2a/b with sterically more demanding $HN(SiMe_2Ph)_2$ (**2**). In $SiMe_2Ph$@SBA-2a (**7**), the sharp OH band at 3695 cm^{-1} exhibits an intensity similar to that of the parent silica (Figure 2D). Furthermore, signals assignable to the phenyl groups of the $\equiv Si-O-SiMe_2Ph$ surface species were scarcely observable. Instead, a small band at 3745 cm^{-1} indicative of pore blocking toward Nujol appeared. The silylation reaction on SBA-2 seems to be limited to the external surface of the silica particles and to the channel entrances (Figure 3).

In accordance with these findings are the microanalytical data (carbon content) and nitrogen adsorption/desorption isotherms of the hybrid materials (Table 1, Figure 4, and Supporting Information, Figure S1). The amount of carbon, found for $SiHMe_2$@SBA-2a/b (**5**/**6**) is considerably smaller than that for $SiHMe_2$@SBA-1 (**3**). This effect is more pronounced for the dimethylphenyl silylated materials: the carbon content of $SiMe_2Ph$@SBA-1 (**4**) is about four times higher than that of $SiMe_2Ph$@SBA-2a/b (**7**/**8**). The N_2 physisorption isotherm of $SiMe_2Ph$@SBA-1 (**4**) revealed a drastic 70% decrease of the total pore volume relative to the unfunctionalized material. The BJH pore diameter dropped from 2.2 to 1.5 nm, and the shape of the isotherm developed from type IV into type I, typical of microporous materials (Figure 4). For the SBA-2 derived hybrid materials the shape of the isotherm did not change.[31−34] The specific pore volume of $SiMe_2Ph$@SBA-2a/b (**7**/**8**) decreased marginally by 10 and 17%, respectively, and the BJH pore diameter remained almost constant. Surface derivatization with dimethylsilyl groups in $SiHMe_2$@SBA-2a/b (**5**/**6**) caused a stronger decrease of the BET surface area and pore volume than the bulkier $SiMe_2Ph$ unit. For SBA-1 materials, the trend is opposite.

Conclusions

Our findings provide strong evidence that the surface reaction of SBA-2 with $HN(SiMe_2Ph)_2$ (**2**) is selective and limited to the external surface of the silica particles. The nonmodified internal surface is anticipated to be accessible to a consecutive functionalization. The vast majority of the channels and pore openings, interconnecting the supercages of SBA-2, displays a diameter larger than the size of a $HN(SiHMe_2)_2$ molecule but smaller than $HN(SiMe_2Ph)_2$. The distinct reaction of $HN(SiHMe_2)_2$ (**1**) with the SiOH groups of SBA-2 can be rationalized on the availability of different channel sizes.[17] SBA-1 features a more open silica framework being fully accessible to both disilazane reagents (Figure 3). Our ongoing work shows that the feasibility of such size/shape selective surface reactions on cagelike mesoporous silicas can be exploited for the development of novel size selective catalysts.

Acknowledgment. We thank the Deutsche Forschungsgemeinschaft and the Fonds der Chemischen Industrie for financial support. This research is also supported by the NANOSCIENCE program of the Universitetet i Bergen.

Supporting Information Available: Figures of physisorption isotherms and BJH pore size distributions of SBA-2b-derived materials (PDF). This material is available free of charge via the Internet at http://pubs.acs.org.

CM0524345

(31) The N_2 physisorption isotherms of SBA-2b parent and silylated materials showed pronounced high-pressure hystereses resulting in bimodal pore size distributions (according to the desorption branch). This is a common phenomenon of cagelike mesoporous silica materials and has been ascribed to the "tensile strength effect"[32] or "spontaneous cavitation" of condensed liquid[29,33] and is depending on the adsorbed gas.[34]

(32) Vinu, A.; Murugesan, V.; Hartmann, M. *Chem. Mater.* **2003**, *15*, 1385.
(33) Thommes, M.; Smarsly, B.; Groenewolt, M.; Ravikovitch, P. I.; Neimark, A. V. *Langmuir* **2006**, *22*, 756.
(34) Kruk, M.; Jaroniec, M. *Chem. Mater.* **2003**, *15*, 1385.